

PROJECT

SEISMIC ANALYSIS OF VOLCANO-TECTONIC ACTIVITY (VT) AT SUNDHNÚKUR, ICELAND: JANUARY 2024

Submission Date: August 1, 2024

Student

Iulia-Ştefania ARMEANU
(Matriculation number: 824289)

Module: GEW-MF12

Course: Volcano Seismology

Lecturer: Prof. Dr. Eva Eibl

Table of Contents

1 Abstract	2
2 Introduction	2
2.1 Eldvörp–Svartsengi volcanic system	2
2.2 2023-24 Sundhnúkur fires	3
2.3 January 2024 - study case	4
3 Theoretical Framework	6
3.1 Volcano-Tectonic events	7
4 Data analysis	7
4.1 Volcano-Tectonic events at Sundhnúkur in January 2024	8
4.2 Comparison between Volcano-Tectonic events type A and type B	9
4.3 Distribution of events in time	11
4.4 Back Azimuth computation	14
5 Conclusion	15
6 References	15

1 Abstract

This report presents a detailed seismic analysis of the volcano-tectonic (VT) events that occurred at Sundhnúkur, Reykjanes Peninsula, Iceland, in January 2024, before and after the eruption on the 14th. Utilizing data from a high broadband seismic station located near the eruption starting point, 6,981 events were automatically detected, with 1,172 verified and categorized into Type A (high frequency, short-duration signals with clear P-wave and S-wave onsets, 1-10 km depth) and Type B (lower frequency, longer-duration signals with emergent P-wave onsets and lacking clear S-wave onsets, <1 km depth) VT events. Multiple clusters of VT events were observed, with significant activity starting on January 3 and another one starting right before the eruption on January 14. Back azimuth analysis indicated a predominant direction of 60°. Particle motion and spectrogram analyses provided further insights into the characteristics and origins of these events. The findings highlight the importance of continuous monitoring and detailed seismic analysis for understanding volcanic behavior and improving eruption prediction.

2 Introduction

Iceland's volcanism includes nearly all volcano types and eruption styles, from mafic lava shields to stratovolcanoes, and from effusive to explosive eruptions. Notably, it features both basaltic and felsic eruptions, including subglacial and phreatomagmatic events, some having global impact (Thordarson and Larsen, 2007). In this study, seismic activity occurring before and after an effusive eruption will be analyzed, including an examination of earthquake patterns and frequencies. This analysis will further provide insights into the precursory and post-eruption seismic signals.

2.1 Eldvörp–Svartsengi volcanic system

In this report, the focus is on the Eldvörp–Svartsengi volcanic system, which comprises fissures, cones, and craters located in southwest Iceland (Figure 1a). This system was chosen for analysis because it was reactivated after approximately 781 years of dormancy, characterized by a series of linear vent systems that ejected lava, tephra, and volcanic gases (Troll et al., 2024).

Svartsengi, on the Reykjanes Peninsula, is a volcanic system known for its geothermal field and energy production at the Svartsengi Power Plant. It lacks a central volcano but includes fissures and high-temperature geothermal fields (Source: Icelandic Institute of Natural History). Eldvörp, located six kilometers west-southwest, was initially considered separate but is now known to be connected, sharing a magma source with Svartsengi (Fulton, C., 2024). Therefore, they are treated as a volcanic system.

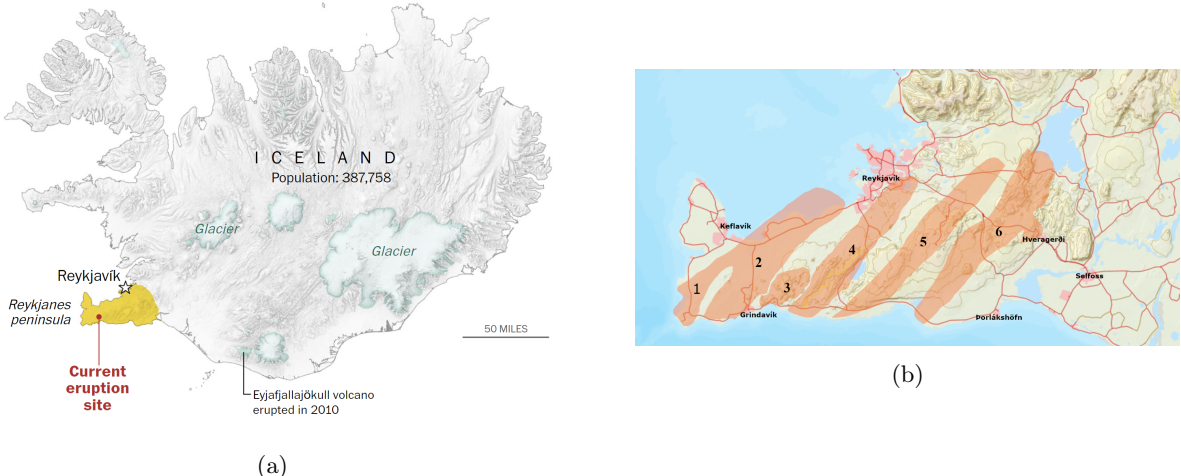


Figure 1: (a) Map of Iceland along with the current eruption site (Source: Washington Post, 2024); (b) Zoom on the RP, showing volcanic lineaments (Source: National Land Survey of Iceland).

The Eldvörp–Svartsengi volcanic system is part of the Reykjanes Volcanic Belt (RVB), located on Reykjanes Peninsula (RP), shown in Figure 1, which is a region of significant volcanic activity, characterized by frequent basaltic eruptions. These eruptions can occur every 3-5 years, with central volcanoes erupting for days to weeks and basaltic fissure eruptions lasting for years. The 2021 eruption on the Fagradalsfjall Volcanic System marked a resurgence of activity, with eight eruptions occurring over the past three years (Troll et al., 2024). The current eruption site is along lineament 2, whereas the 2021 Fagradalsfjall eruption took place along lineament 3 (Figure 1b).

According to Parks et al., 2024, this reactivation was not unexpected due to the historical pattern of volcanic activity on RP, with intervals between eruptive periods averaging 800-1000 years. The reactivation began in December 2019, with four dike intrusions and three eruptions in both the Fagradalsfjall and Svartsengi areas. Increased seismicity and ground deformation indicated magma accumulation, leading to significant eruptions from 2021 to 2023 (Parks et al., 2024), and continuing into 2024. As shown in Figure 2, the eruptions in 2024, starting with the eruption on January 14th (analyzed in this report), resulted in lava flows that were closer to the city of Grindavík, the Blue Lagoon, and the Svartsengi Power Plant compared to the 2021-2023 eruptions. This increased proximity posed additional risks to these key locations, highlighting the importance of continuous monitoring and hazard assessment.

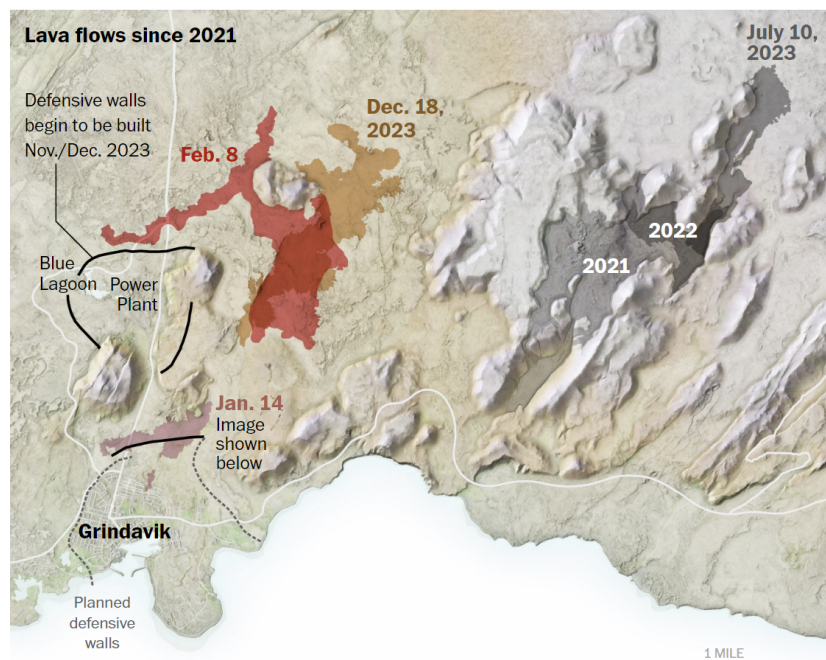


Figure 2: A detailed map of lava flows since 2021, focusing on the area around Grindavík, the Blue Lagoon, and the Power Plant in Iceland, including information about defensive walls planned to be built in November/December 2023. (Source: Washington Post, 2024)

2.2 2023-24 Sundhnúkur fires

Figure 3 provides a detailed visualization of the volcanic events and their impacts as discussed in this section. The map shows critical and insightful information, particularly for this study, including the eruptive fissures and the extent of lava flows from the 2023-2024 eruptions, which directly affected the nearby areas, including Grindavík and the Blue Lagoon.

According to the Icelandic Met Office, volcanic activity at Sundhnúkur began with magma accumulation at a depth of 4-5 km beneath Svartsengi at the end of October 2023. This initial phase was detected through increased seismicity, with a swarm consisting of over 10,500 earthquakes, over 26 of which exceeded magnitude three, and significant ground deformation. The latest satellite radar image, acquired on October 31, revealed ground movement of 5 to 6 cm over 12 days, centered just northwest of Mt. Porbjörn, situated between Grindavík and the Blue Lagoon (blue triangle in Figure 3) (Icelandic Met

Office, 2024; Troll et al., 2024).

Subsequently, a major earthquake swarm on November 10, 2023, signaled the movement of magma and further destabilized the region. The seismic activity moved south towards Grindavík. Based on the evolution of the seismic activity that day, along with results from GPS measurements, it was likely that a magma intrusion extended beneath Grindavík, leading to the evacuation of the town (Icelandic Met Office, 2024).

The first eruption occurred between December 18-21, 2023, resulting in a substantial lava field covering 3.4 km². This marked the beginning of a series of volcanic events. The second eruption, from January 14-16, 2024, produced a smaller lava field but brought the lava flow dangerously close to populated areas, including the town of Grindavík, the Blue Lagoon, and the Svartsengi Power Plant. This proximity posed significant risks to infrastructure and local communities, necessitating the construction of defensive walls to mitigate lava flow impacts (Baisas, L., 2024).

A third eruption followed on February 8, 2024, further expanding volcanic activity in the region. The fourth eruption on March 16, 2024, added to the complexity of the situation, with each eruption varying in lava field extent and posing unique challenges for monitoring and response efforts (Icelandic Met Office, 2024; Icelandic Institute of Natural History).

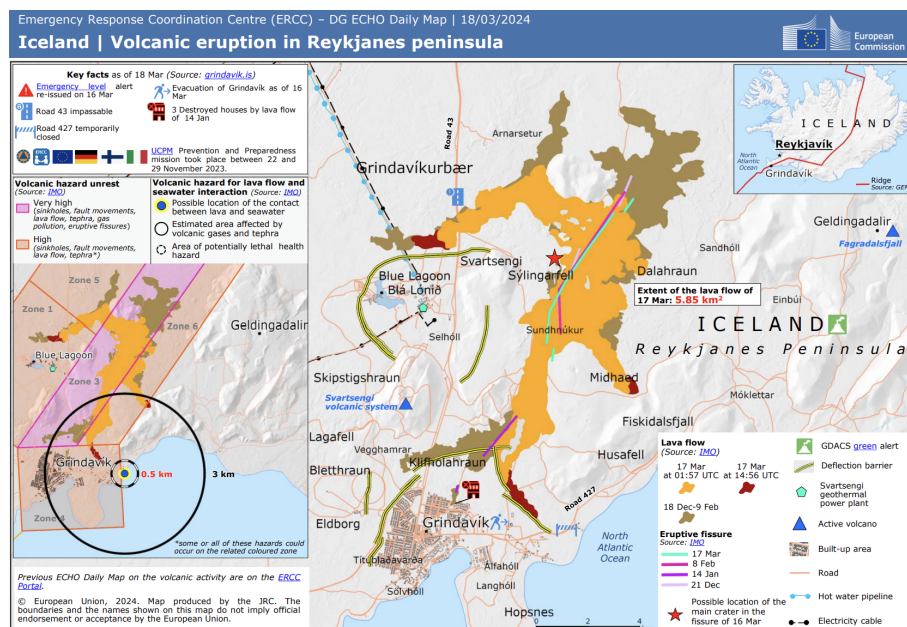


Figure 3: The volcanic eruption and seismic activity in RP, highlighting key affected areas (Grindavík, the Blue Lagoon, and the Svartsengi Power Plant), the extent of lava flows from the 2023-2024 eruptions, ground deformation, and the deflection barrier.
(Source: Emergency Response Coordination Centre (ERCC), 2024)

The ongoing volcanic activity at Sundhnúkur highlighted the dynamic nature of the RP volcanic systems and underscored the importance of continuous monitoring, hazard assessment, and preparedness to protect local communities and critical infrastructure from the impacts of volcanic eruptions.

2.3 January 2024 - study case

The effusive volcanic eruption on January 14, 2024, commenced at 07:57 UTC, southeast of Hagafell mountain, approximately 900 meters from Grindavík. As depicted in Figure 4, lava flowed towards Grindavík, south of the newly constructed deflection barriers. The eruption's onset was characterized by intense seismic activity at the Sundhnúkgígar crater row, which initiated around 03:00 UTC on January 14, 2024, with a significant magnitude 3.5 earthquake near Hagafell at 04:07 UTC marking a shift in

seismicity towards Grindavík, indicative of magma movements beneath the surface (Icelandic Met Office, 2024; EGU Blogs, 2024).

Additionally, on the same day at 12:10 UTC, another eruptive fissures formed, approximately 100 meters in length, resulting in substantial lava flow reaching Grindavík and igniting at least three houses (see Figure 4). By 16:40 UTC on January 15, the activity at this shorter fissure had ceased, and the effusion rate at the primary fissure had significantly decreased. The main fissure ceased lava effusion around 01:00 UTC on January 16 (Icelandic Met Office, 2024; Global Volcanism Program, Iceland, Weekly Reports, 2024).

Notably, on January 3, at 10:50 AM, a 4.5 magnitude earthquake occurred near Trölladyngja (about 20 kilometers north-northeast of Svartsengi and Grindavík), followed by a 3.9 magnitude quake at 10:54 AM and over 900 aftershocks at depth of about 5 km. According to Icelandic Met Office, these events were likely triggered by stress release from earth movements on the RP, but there is no indication that these earthquakes are directly linked to magma movements.

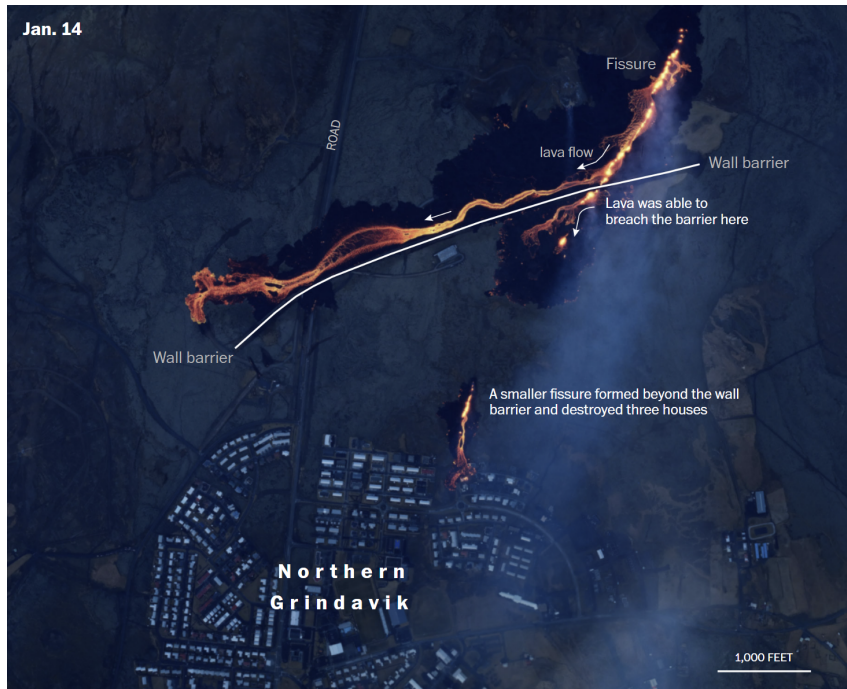


Figure 4: The two fissures occurred in January near Grindavík, showing the lava flow along with the wall barrier that was constructed to protect the city. (Source: Washington Post, 2024)

According to recent studies on volcanic activity in the RP (Páll Einarsson, 2018; Victor M. Hernández-Aguirre et al., 2023), eruptions are typically preceded by intense seismic swarms, indicating the upward movement of magma through the crust. The pattern of this eruption aligns with these observations, demonstrating the critical interplay between seismic activity and volcanic events.

Thus, this study focused on the Volcano-Tectonic (VT) events recorded during January 2024, using data from nearby seismic stations. The map in Figure 5 displays the central position of the eruption studied in this report and the previous one in December, along with the seismic stations used for data analysis. Station SAND was utilized for waveform analysis, spectral characteristics, and particle motion computations, while station SVA, incorporating rotational sensor, was used for back azimuth analysis.

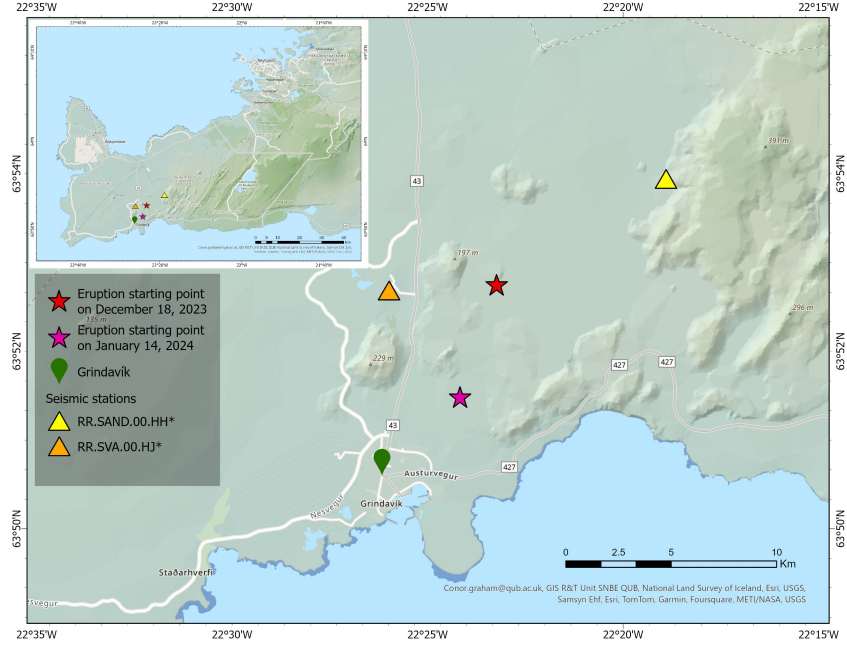


Figure 5: Map showing the eruption starting points near Grindavik, with the red star marking the eruption starting point on December 18, 2023, and the purple star marking the eruption starting point on January 14, 2024 (the one analyzed in this report), along with the seismic stations used in this study and surrounding geographic features.

3 Theoretical Framework

Seismological observations are crucial for monitoring and forecasting volcanic eruptions, as nearly all such eruptions show seismic anomalies beforehand. These anomalies are detected by counting volcanic events and analyzing their hypocenter distributions. However, the relationship between seismic events and ascending magma remains unclear, partly due to the varied terminology for volcano-seismic events (IASPEI, Chapter 13). As shown in Figure 6, various seismic events around volcanoes play critical roles in understanding volcanic mechanisms. This study focuses on Volcano-Tectonic (VT) events, further categorized as Type A and Type B based on their properties.

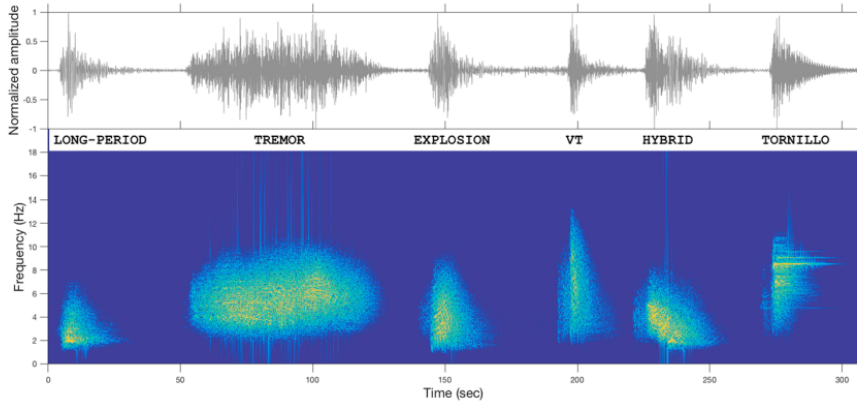


Figure 6: Waveform and spectrogram (Gaussian window of 512 samples width) recorded at Ubinas Volcano, showing different types of volcano seismic signals (Source: Marielle Malfante et al., 2018).

3.1 Volcano-Tectonic events

Volcano-tectonic (VT) events are seismic activities caused by magma or volcanic fluid movements within the Earth's crust, categorized into Type A and Type B based on their seismic characteristics and mechanisms (Chouet and Matoza, 2013; IASPEI, Chapter 13).

Type A VT events (see Figure 7a) feature high-frequency seismic waves (>5 Hz) with well-defined P-wave and S-wave onsets, short signal durations, and depths of 1-10 km, indicating rapid rock fracturing. These characteristics make them easier to identify and analyze. Type B VT events (see Figure 7b) have lower frequency waves (1-5 Hz), long signal durations, emergent P-wave onsets, and typically lack S-wave onsets. They occur at shallower depths (<1 km) and are associated with slower processes like fluid movement and gas pressure buildup (IASPEI, Chapter 13).

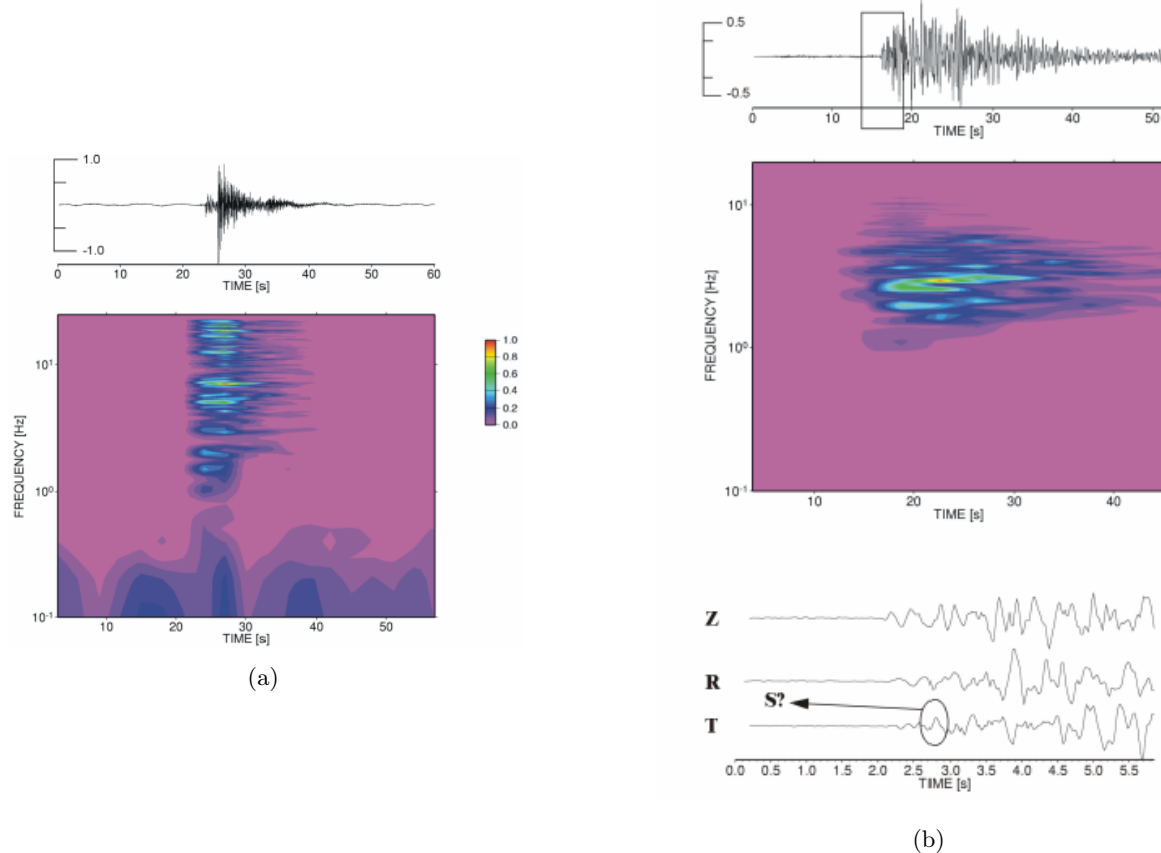


Figure 7: (a) Example of VT-A type event recorded at Mt. Merapi, Indonesia.
 (b) Example of VT-B type event recorded at Mt. Merapi, Indonesia, along with a zoom-in on the S wave to show that no clear peak can be recognized (Source: IASPEI, Chapter 13).

4 Data analysis

The study spanned from January 1 to 31, 2024, utilizing high broadband stations with a 200 Hz sampling rate. The STA/LTA (Short-Term Average/Long-Term Average) method, integrated within the open-source Pyrocko Snuffler tool (Heimann S., et al., 2017), was employed for efficient processing and analysis of the large seismic dataset, ensuring accurate identification of significant seismic activities. The STA/LTA method compares the average signal amplitude over a short time window (STA) with that over a longer time window (LTA), detecting a seismic event when the ratio of these averages exceeds a predefined threshold.

As illustrated in Figure 8, a 5-15 Hz bandpass filter was used for this analysis, with a short window of 3 seconds, a ratio of 3.5, and a level of 0.7. These parameters were selected after several trials to avoid

detecting long-period events or high-frequency spikes from different sources.

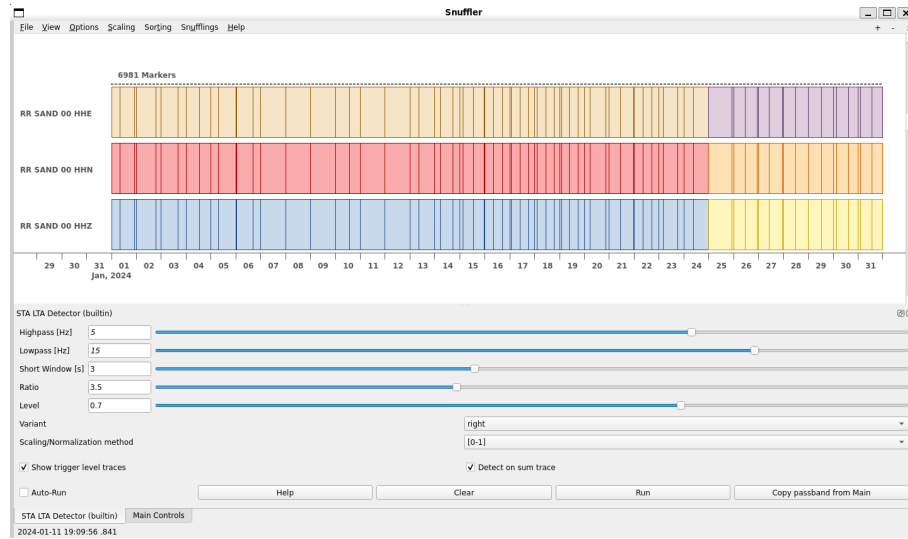


Figure 8: Snuffler interface of STA/LTD detector, showing the parameters used for automatic detection in this study. The picture, taken after applying the tool, displays the number of automatically detected events in the upper left corner.

Firstly, for waveform visualization, spectrogram characteristics, and particle motion computation, data streams from different components (Z, N, and E for the SAND station - see Figure 5) were read and combined. All waveforms, along with the spectrogram, were analyzed to classify different types of events as accurately as possible. The dataset was pre-processed by trimming, detrending, tapering, and applying instrument response correction. A bandpass filter of 5-15 Hz was applied, followed by further trimming to isolate the event signal. For waveform and spectrogram analysis, a length of 30 seconds was used: 10 seconds before the P-wave arrival and 20 seconds after. For particle motion computation, a 3-second length after the P-wave arrival was used.

Additionally, back-azimuth (BAZ) calculations using 3 component rotation sensors from SVA station (see Figure 5) were performed using the method described by Yuan et al. (2020), and modified by Eva Eibl. This involved reading rotation rate data and synchronizing it with acceleration data. The analysis utilized the covariance matrix and eigenvalue decomposition to determine the BAZ, while addressing the 180-degree ambiguity by comparing rotated transverse components with vertical acceleration components. The data streams were merged, trimmed, detrended, and filtered with a 5-15 Hz bandpass filter to prepare for BAZ analysis. This analysis provided insights into the directionality of seismic events and enhanced the overall understanding of the volcanic activity being studied.

4.1 Volcano-Tectonic events at Sundhnúkur in January 2024

In this study, Type A VT events are characterized as detailed in Section 3. Conversely, Type B VT events exhibit characteristics similar to either Explosion or Hybrid events (see Figure 6). Further, events will be referred to as Type A and Type B to distinguish between different waveforms, but it is important to note that Type B VT events start with higher frequency, followed by low-frequency content, longer-duration signals, and less-defined waveforms. They also feature an emergent P-wave onset and lack a clear S-wave.

The automatic detection tool STA/LTA identified 6,981 events, which were manually verified to confirm 1,172 events (890 Type A and 282 Type B). Additional events were detected, but no events were missed, demonstrating the tool's efficiency when combined with manual verification. During manual verification, only signals occurring on all components were considered. During the manual verification, P and S arrival times were picked.

4.2 Comparison between Volcano-Tectonic events type A and type B

In this part of the analysis the focus is on distinguishing between Type A and Type B VT events based on their waveform characteristics, spectrograms, and particle motions.

Firstly, eight random events from each type were chosen. Type A events can be seen in Figure 9 and Type B in Figure 10. Both event types exhibit high-frequency content, with Type B events showing this characteristic primarily at the beginning, followed by lower frequency content. The duration of Type B events is longer, with a larger P-wave visible at the beginning. When comparing these observations with the literature presented in Section 3, it becomes evident that, at this particular volcano, the Type B events resemble more closely Hybrid or Explosion events.

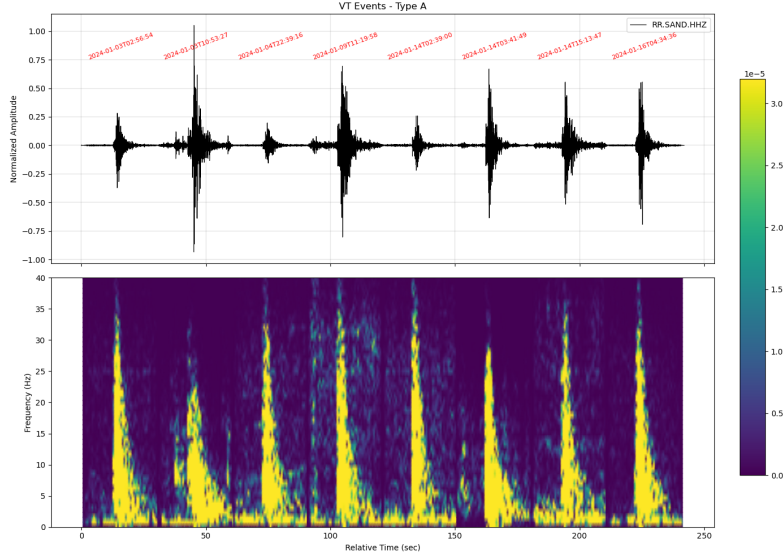


Figure 9: Eight random events of Type A plotted together. The time of each event (P arrival) can be seen at the top of each waveform. Only vertical component (HHZ) is shown in the first plot, and the second one displays the corresponding spectrograms.

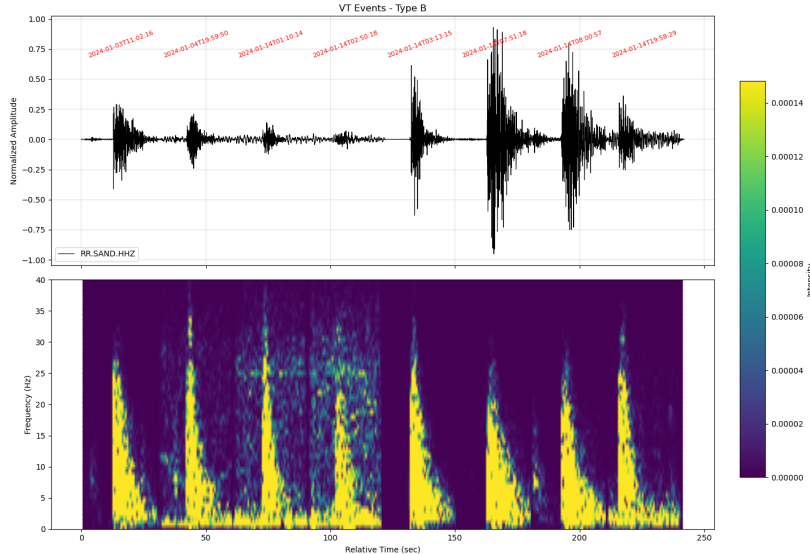


Figure 10: Eight random events of Type B plotted together. The time of each event (P arrival) can be seen at the top of each waveform. Only vertical component (HHZ) is shown in the first plot, and the second one displays the corresponding spectrograms.

To gain a more detailed understanding, one event from each type was further analyzed. The event on February 14 at 03:41:49 UTC was used for Type A (Figure 11(a,c,e)), and the event on February 14 at 08:24:08 UTC was used for Type B (Figure 11(b,d,f)). Both events occurred in close proximity to the eruption on February 14 at 07:57 UTC (first and larger fissure).

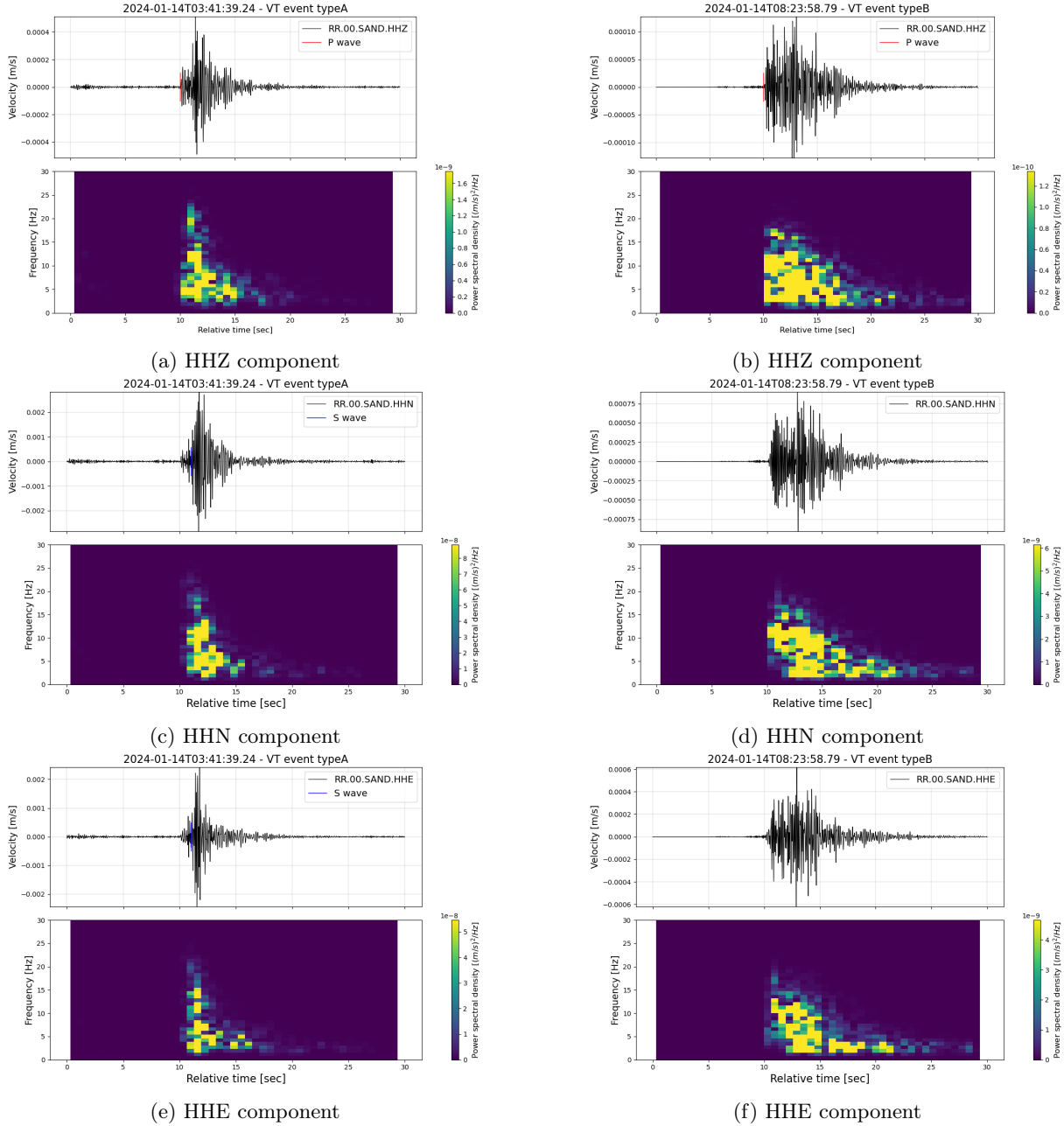


Figure 11: Comparison between type A and type B VT events using waveform and spectral characteristics for each component. The event of type A is shown in figures: (a), (c), (e). The event of type B is shown in figures: (b), (d), (f). The time written at the top of each plot represents the starting time of the plot.

For Type A event (Figure 11(a,c,e)), high-frequency seismic waves with clear P-wave and S-wave onsets are observed, with higher amplitudes in the horizontal components (HHE and HHN) compared to the vertical component (HHZ), which is typical for tectonic events. The duration of the signal is approximately 5 seconds. The spectrograms show a concentration of energy at higher frequencies (1-15 Hz) during the initial phase of the event, indicating the high-frequency nature of Type A events.

For VT Event Type B, as seen in Figure 11(b,d,f), the events are characterized by lower frequency waves, but a high-frequency content can be seen at the beginning of the signal. They have longer signal duration of approximately 10 seconds and emergent P-wave onsets without clear S-wave onsets. The spectrograms indicate the presence of lower frequency content (1-10 Hz) throughout the duration of the event. Unfortunately, the depth cannot be computed with just one station, so it cannot be determined at which depth the two types occurred. Depth analysis can only be performed for Type A events by computing the P-S time difference, which will be analyzed later.

The particle motion plots provide valuable insights into the characteristics of VT events Type A and Type B (see Figure 12). For VT Event Type A (Figure 12(a)), the particle motion plots display elliptical patterns in the horizontal plane (HHE-HHN) and linear patterns in the vertical planes (HHZ-HHE and HHZ-HHN). These patterns indicate clear P-wave polarization and subsequent S-wave shear motion, typical of tectonic events. In contrast, VT Event Type B (Figure 12(b)) shows scattered patterns in the horizontal plane, indicating a less coherent wavefield possibly associated with fluid movements. However, the vertical planes exhibit similar linear patterns to Type A events, reflecting consistent vertical P-wave propagation. Overall, Type A events exhibit organized, clear patterns reflecting tectonic fracturing, while Type B events show disorganized, scattered horizontal patterns.

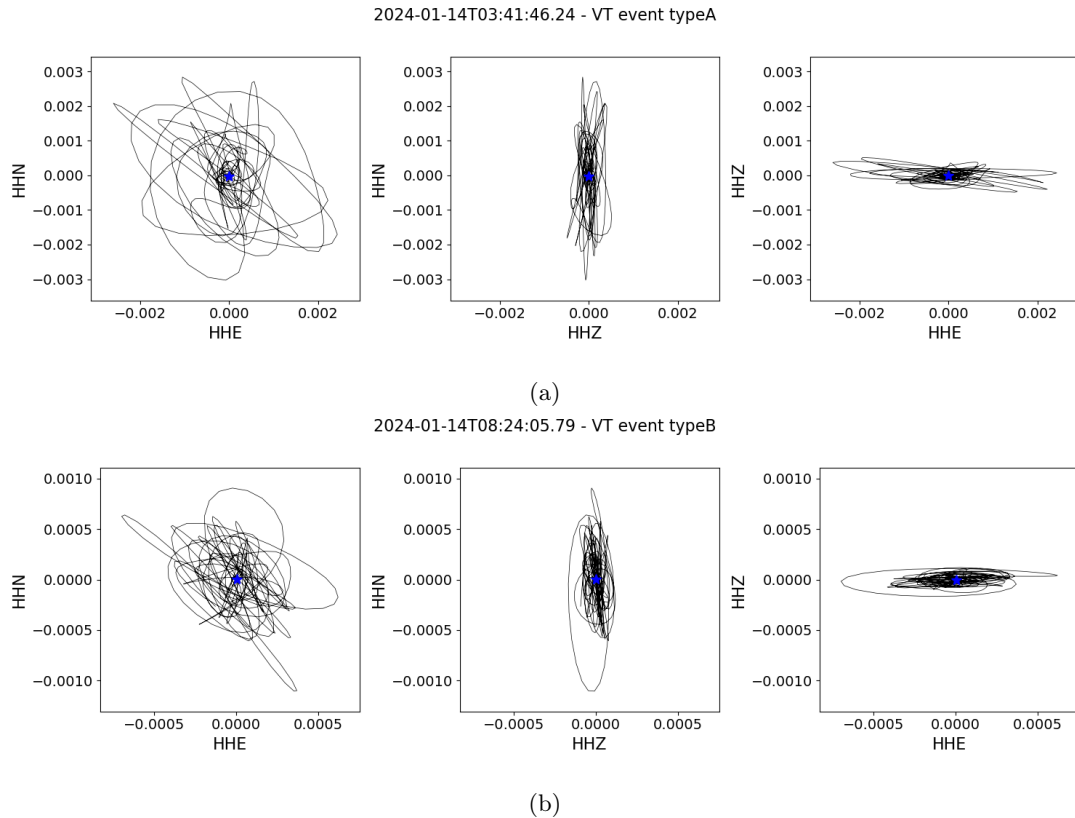


Figure 12: Particle motion plots for VT Event Types A and B. The time written at the top of each plot represents the starting time of the plot.

4.3 Distribution of events in time

Further in analyzing the events that occurred in January 2024 at Sundhnúkurgígar, Iceland, the distribution of events over time was examined using P-wave arrivals for both types of VT events and S-wave arrivals for Type A VT events.

Firstly, the frequency of events was analyzed (see Figure 13). The plot shows the number of events each day along with the hourly distribution of events throughout the day. The plot reveals two clusters of events. The first cluster occurs within the first five days of January, peaking on January 3. This is consistent with observational data from the Icelandic Met Office (see Section 2.3), which describes a swarm of events starting on January 3. Some of these events are connected to the swarm, though it

is not entirely clear if they are directly linked to the eruption. It is also interesting to note that most of the Type B VT events occur right before, during, and immediately after the eruption. This was expected, as these events are either associated with sudden magma extrusion, ash and gas emission, or fluid movements (Marielle Malfante et al., 2018). The second cluster starts right before the eruption (marked by a black star in Figure 13) and continues until the beginning of January 16. This pattern is consistent with the literature data presented in Section 2.3. After the eruption, the seismicity began to calm down. Additionally, on January 14, there are no specific events that can be associated with the second fissure. However, since that fissure is further from the station used in this study, only the main fissure will be discussed.

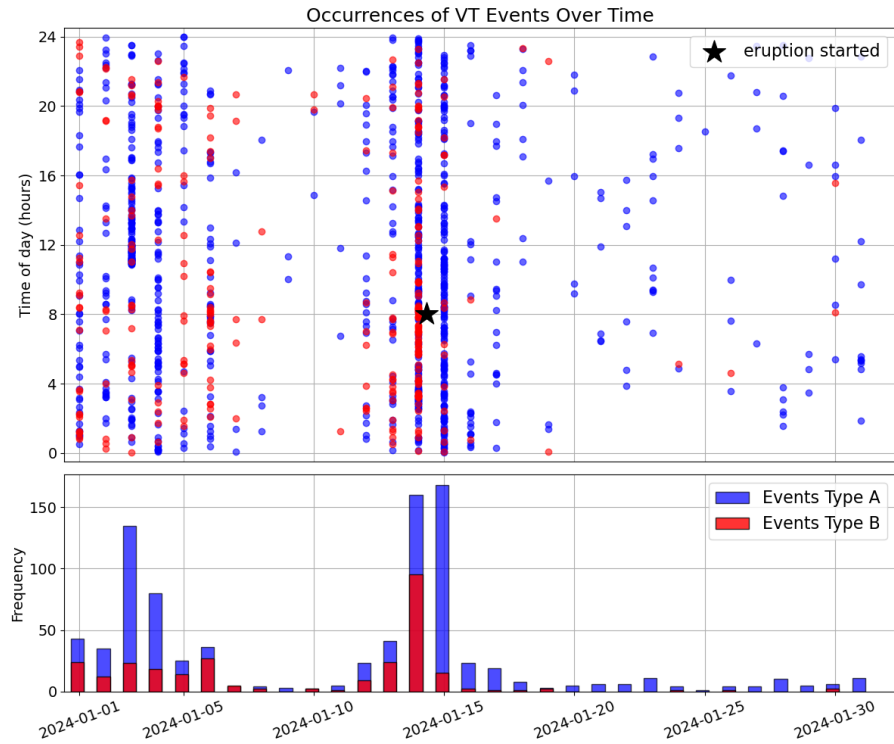


Figure 13: Temporal distribution of VT events in January 2024. The top plot shows the occurrences of VT events over time, with blue dots for Type A and red dots for Type B events. The black star marks the eruption on January 14. The bottom plot shows the daily frequency of VT events, with blue bars for Type A and red bars for Type B events.

Secondly, to better understand the nature of these events, the depth of the events was inferred from the P-S time differences, with shorter times indicating shallower depths and longer times indicating deeper events. Thus, the P-S time differences were plotted against P arrival (considered here as the origin time of the events), and the result is shown in Figure 14. The analysis revealed three clusters:

1. A well-defined cluster around January 3 with longer P-S times between 1.75 and 2.25 seconds, indicating deeper events. This cluster likely represents the seismic swarm observed on January 3.
2. A cluster with P-S time differences between 0.5 and 1.5 seconds from January 1 to January 7, which can be associated with the pre-eruption activity. This pattern is similar to the third cluster, which shows P-S times not exceeding 1.75 seconds.
3. The third cluster, occurring around the eruption on January 14, shows similar P-S times to the second cluster, indicating shallow depths.

The presence of shallower events before the eruption suggests that the seismic swarm might be a result of triggered seismicity by volcanic activity rather than indicating magma movement. After the eruption, most events continued to occur at shallow depths, with only a few occurring at greater depths.

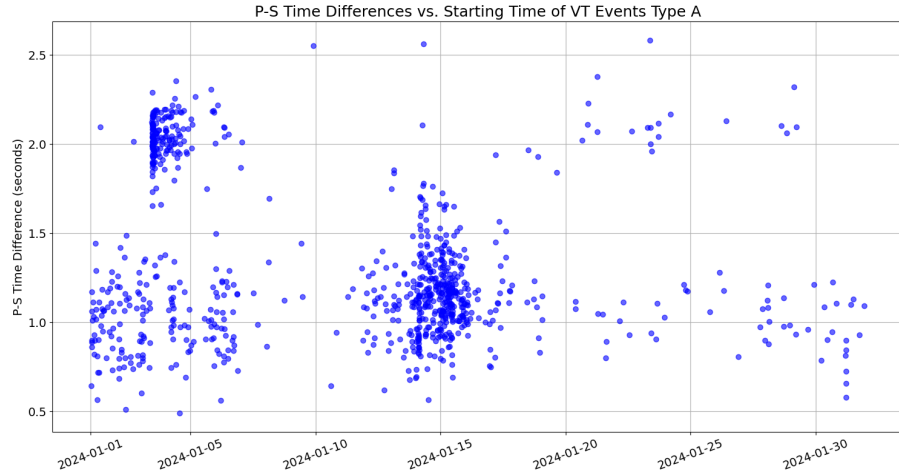


Figure 14: P-S time differences vs. starting time of VT Events Type A in January 2024. The plot shows the P-S time differences (in seconds) on the y-axis against the starting time of the events on the x-axis (P arrival).

Upon examining closer the seismic data from January 14 (see Figure 15), it is evident that there are no signs indicating the presence of a second fissure. The seismic records show that amplitudes are significantly higher just before the eruption, especially marked by the 3.5 ML quake at the 4-hour mark. This pattern of increased seismic activity before an eruption is consistent with the understanding that the movement of magma and volcanic gases causes many small earthquakes as it forces the surrounding rocks to crack (Katharine Solada and K. Sean Daniels, 2021). During the eruption, the amplitudes decrease, which is typical as the pressure is released.

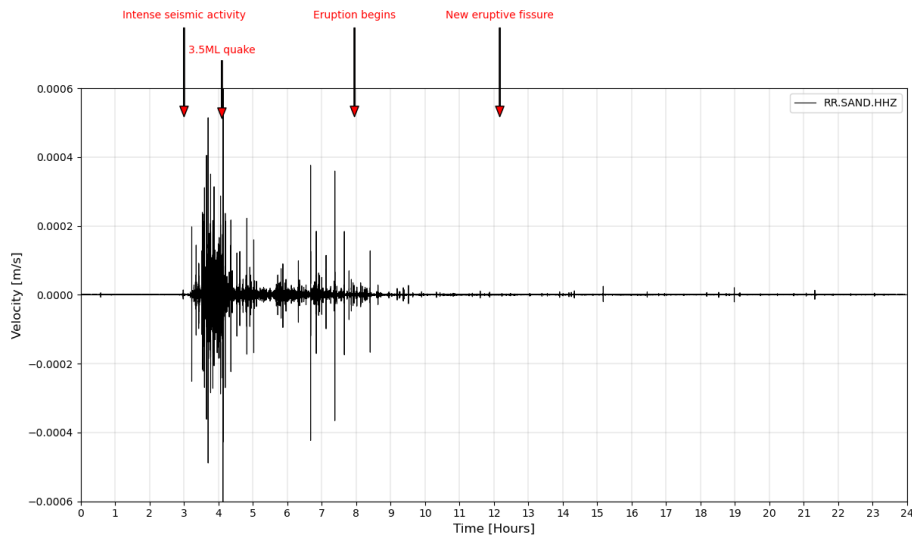


Figure 15: Seismic activity recorded over a 24-hour period in January 14, 2024 at station SAND.

Analyzing seismic sequences like the one starting early on January 14 and culminating in the 3.5 ML event can be very useful for predicting volcanic eruptions. However, this analysis does not provide clear information about the duration of eruption, but that can be inferred from a decrease in seismicity. The only noteworthy observation during an eruption is the occurrence of type B seismic events, which might indicate ongoing volcanic activity and the movement of magma. These findings highlight the importance of continuous seismic monitoring and the need for integrated analysis using multiple data types, including seismicity, ground deformation, and gas emissions, for more accurate eruption forecasting.

4.4 Back Azimuth computation

Back azimuth (BAZ) computation provides directional information of seismic events using data from a single 3-component seismic station. The back azimuth is the angle from the station to the seismic source, measured clockwise from North. By analyzing the vector of P-wave motion, which is polarized in the vertical plane of propagation, it can be decomposed into vertical and radial components to calculate the BAZ. The radial component of the P-wave is reconstructed from the two horizontal seismometer components (N-S and E-W). Correct interpretation of the first motion polarity ensures accurate BAZ determination, which is crucial for understanding the source direction of seismic events (IASPEI, Earthquake location).

For this analysis, two events were chosen: one of Type A (see Figure 16) and one of Type B (see Figure 17), both occurring on the day of the eruption. The consistent directional information obtained enhances the understanding of the source dynamics and propagation characteristics of seismic waves during volcanic eruptions.

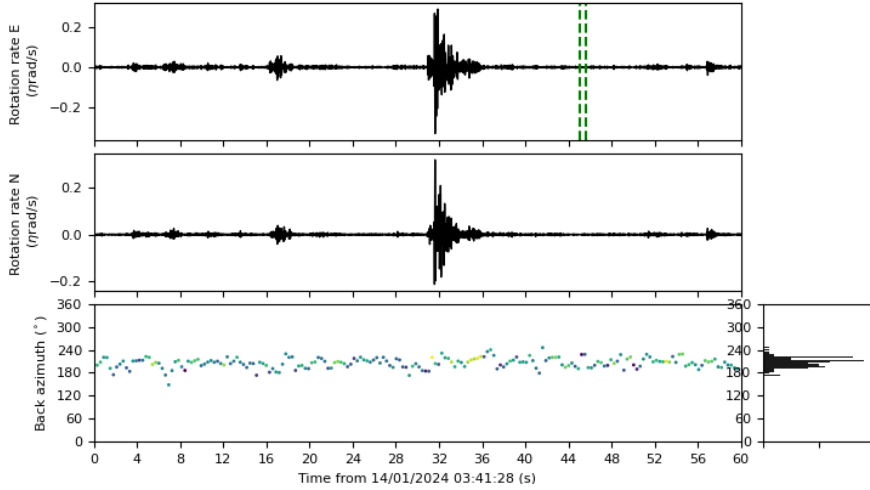


Figure 16: Seismic event Type A showing the reduction rates in the E and N components and the back azimuth over time. The green lines indicate the window length used for the computation.

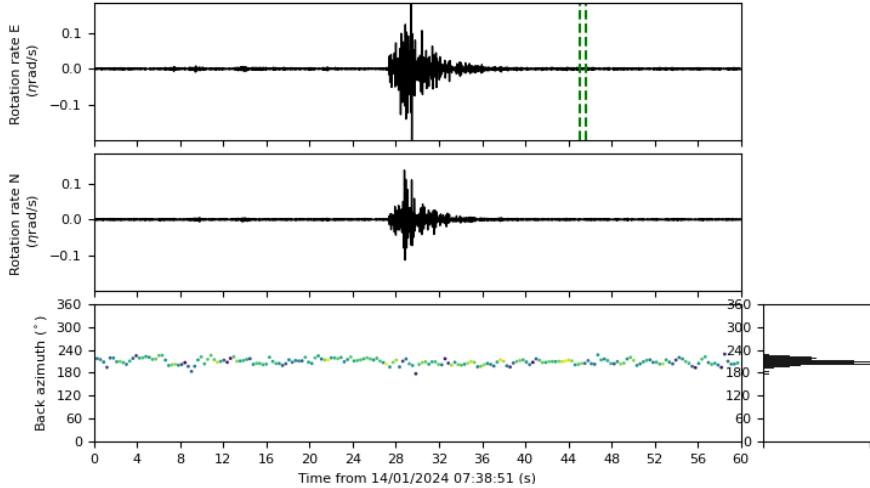


Figure 17: Seismic event Type B showing the reduction rates in the E and N components and the back azimuth over time. The green lines indicate the window length used for the computation.

In the analysis, the back azimuth computations revealed a predominant direction around 220° (southwest) for both Type A and Type B events. The histogram on the right side of the BAZ plot indicates

the distribution of BAZ values during the window, confirming the stability of the direction around 220°. However, there is a 180° ambiguity in this calculation due to the polarity of the first motion of the P-wave. This means that the BAZ could alternatively be 60° (northeast).

By considering the location of the seismic station and the data provided by the Icelandic Met Office, it is more probable that the correct BAZ is around 60°. This is supported by the location of the eruption center and the station location SVA, as depicted in Figure 5. The consistent directional information obtained enhances the understanding of the source dynamics and propagation characteristics of seismic waves during volcanic eruptions.

5 Conclusion

This study presents a comprehensive seismic analysis of volcano-tectonic (VT) events at Sundhnúkurgígar, Iceland, during January 2024, providing valuable insights into the seismic behavior preceding, during, and following a significant volcanic eruption on January 14. The analysis utilized data from high broadband seismic stations, enabling the detection, verification, and classification of 1,172 VT events into Type A and Type B.

The temporal distribution of VT events showed two main clusters. The first cluster, around January 3, coincides with a seismic swarm, indicating increased volcanic activity. The second cluster, starting just before the eruption and continuing until January 16, underscores the relationship between increased seismicity and volcanic eruptions. As a key finding, the clustering of VT events that was observed before the eruption, starting on January 3, might not be related to magma movement, and be instead just a swarm that was triggered by the volcanic activity.

Analysis of seismic activity on January 14 revealed a significant increase in seismic amplitudes just before the eruption, marked by a 3.5 ML earthquake. This pattern is consistent with the movement of magma and volcanic gases causing small earthquakes as the surrounding rocks crack. During the eruption, seismic amplitudes decreased, indicating pressure release.

Back azimuth computations indicated a predominant direction around 220° (southwest), later interpreted as 60° (northeast) based on station location and eruption center data.

Overall, this study emphasizes the dynamic nature of volcanic systems and the necessity of integrated monitoring approaches, combining seismicity, ground deformation, and gas emissions data, for accurate forecasting and hazard assessment. The continuous analysis and monitoring of VT events at Sundhnúkurgígar and other similar volcanic systems are crucial for enhancing our understanding of volcanic processes and improving public safety.

Additionally, future work could focus on examining the correlation between Type A and Type B events to determine whether they originate from the same or different sources. Furthermore, creating templates of waveforms could be beneficial for identifying and categorizing more events with greater accuracy.

6 References

1. Baisas, L. (2024, June 26). Iceland's 'unparalleled' volcanic activity could continue for decades. Popular Science. Accessed July 2024 from [link](#)
2. Bormann, P. (Ed.). (2012). New Manual of Seismological Observatory Practice (NMSOP-2). Potsdam: Deutsches GeoForschungszentrum GFZ; IASPEI. <https://doi.org/10.2312/GFZ.NMSOP-2>
3. Chouet, B. A., & Matoza, R. S. (2013). A multi-decadal view of seismic methods for detecting precursors of magma movement and eruption. Journal of Volcanology and Geothermal Research, 252(Supplement C), 108–175, <https://doi.org/10.1016/j.jvolgeores.2012.11.013>

4. EGU Blogs. (2024). Details on the January 2024 Eruption in Iceland. European Geosciences Union.
5. Einarsson, P. (2018). Seismicity and Magmatic Activity in the Reykjanes Peninsula. *Journal of Volcanology and Geothermal Research*, 341, 100-110.
6. Emergency Response Coordination Centre (ERCC). (2024, March 18). Iceland: Volcanic eruption on Reykjanes Peninsula - DG ECHO Daily Map. ReliefWeb. Accessed August 1, 2024, from [link](#)
7. Fulton, C. (2024, January 10). So, what happens now? Perspectives on the future of the Reykjanes Peninsula. The Reykjavik Grapevine. Accessed from [link](#)
8. Global Volcanism Program. (2024). Iceland Weekly Volcanic Activity Reports. Smithsonian Institution.
9. Heimann, S., Kriegerowski, M., Isken, M., Cesca, S., Daout, S., Grigoli, F., Juretzek, C., Megies, T., Nooshiri, N., Steinberg, A., Sudhaus, H., Vasyura-Bathke, H., Willey, T., Dahm, T. (2017): Pyrococko - An open-source seismology toolbox and library, Potsdam : GFZ Data Services., <https://doi.org/10.5880/GFZ.2.1.2017.001>
10. Hernández-Aguirre, V. M., et al. (2023). Magma Movement and Seismic Activity in Iceland. *Geophysical Research Letters*, 150(7), 987-1002.
11. Icelandic Institute of Natural History. (n.d.). Volcanic activity. Accessed from <https://www.ni.is/en/geology/volcanic-activity>, Accessed July 2024.
12. Icelandic Meteorological Office. (2024, July 30). Increased probability of a dike propagation and a volcanic eruption in the coming days, Accessed July 2024 from [link](#)
13. Marielle Malfante, Mauro Dalla Mura, Jerome I. Mars, Jean-Philippe Métaxian, Orlando Macedo, et al.. Automatic classification of volcano seismic signatures. *Journal of Geophysical Research*, 2018, 123 (12), pp.10,645-10,658. doi: 10.1029/2018jb015470
14. National Land Survey of Iceland. (n.d.). Reykjanes volcanic systems [Map]. Accessed August 1, 2024, from https://commons.wikimedia.org/wiki/File:Reykjanes_volcanic_systems.png
15. Parks, M., Sigmundsson, F., Barsotti, S., Geirsson, H., Vogfjörð, K. S., Ófeigsson, B., Einarsson, P. (n.d.). Fagradalsfjall eruption. Icelandic Meteorological Office. Accessed August 1, 2024, from <https://en.vedur.is/volcanoes/fagradalsfjall-eruption/>
16. Solada, K., & Daniels, K. S. (2021). Principles of Earth Science. Open Oregon Educational Resources. Accessed August 1, 2024, from <https://openoregon.pressbooks.pub/earthscience/>
17. The Washington Post, Volcano Eruption in Iceland near Grindavik. (2024, February 8). Accessed from [link](#), Accessed July 2024.
18. Thordarson, T. and Hoskuldsson, A. (2008). Postglacial volcanism in Iceland. *Jokull*, 58(1). <https://doi.org/10.33799/jokull2008.58.197>
19. Troll, V. R., Deegan, F. M., Thordarson, T., Tryggvason, A., Krmíček, L., Moreland, W. M., Lund, B., Bindeman, I. N., Höskuldsson, Á., Day, J. M. D. (2024). The Fagradalsfjall and Sundhnúkur Fires of 2021–2024: A single magma reservoir under the Reykjanes Peninsula, Iceland? *Terra Nova*. <https://doi.org/10.1111/ter.12733>
20. Yuan, S., Simonelli, A., Lin, C. J., Bernauer, F., Donner, S., Braun, T., et al. (2020). Six degree-of-freedom broadband ground-motion observations with portable sensors: Validation, local earthquakes, and signal processing. *Bulletin of the Seismological Society of America*, 110(3), 953–969. <https://doi.org/10.1785/0120190277>